ACS APPLIED MATERIALS & INTERFACES

Research Article

www.acsami.org

Dramatic Improvement in Water Retention and Proton Conductivity in Electrically Aligned Functionalized CNT/SPEEK Nanohybrid PEM

Swati Gahlot[†] and Vaibhav Kulshrestha*[,†,‡]

[†]CSIR-Central Salt and Marine Chemicals Research Institute (CSIR-CSMCRI), Council of Scientific & Industrial Research (CSIR), Gijubhai Badheka Marg, Bhavnagar- 364 002, Gujarat, India

[‡]Academy of Scientific and Innovative Research, Council of Scientific & Industrial Research (CSIR), Gijubhai Badheka Marg, Bhavnagar- 364 002, Gujarat, India

Supporting Information

ABSTRACT: Nanohybrid membranes of electrically aligned functionalized carbon nanotube *f* CNT with sulfonated poly ether ether ketone (SPEEK) have been successfully prepared by solution casting. Functionalization of CNTs was done through a carboxylation and sulfonation route. Further, a constant electric field (500 V·cm^{-2}) has been applied to align CNTs in the same direction during the membrane drying process. All the membranes are characterized chemically, thermally, and mechanically by the means of FTIR, DSC, DMA, UTM, SEM, TEM, and AFM techniques. Intermolecular interactions between the components in hybrid membranes are established by FTIR. Physicochemical measurements were done to analyze membrane stability. Membranes are evaluated for proton conductivity (30−90 °C) and methanol crossover resistance to reveal their potential for direct methanol fuel cell application. Incorporation of *f* CNT reasonably increases the ion-exchange capacity, water retention, and proton conductivity while it reduces the methanol permeability. The maximum proton conductivity has been found in the S-sCNT-5 nanohybrid PEM with higher methanol crossover resistance. The prepared membranes can be also used for electrode material for fuel cells and batteries.

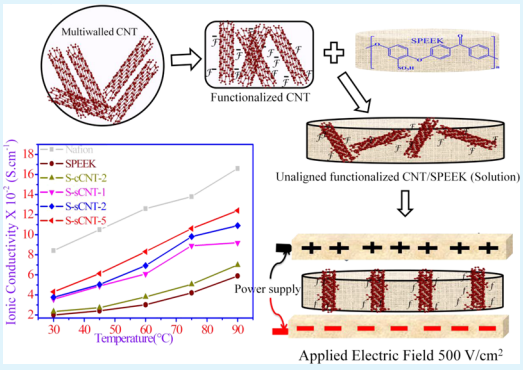

KEYWORDS: *poly ether ether ketone, functionalized carbon nanotube, PEMs, proton conductivity, electronic conductivity, thermo-mechanical stability*

INTRODUCTION

Proton exchange membranes (PEMs) are widely used in different applications, such as fuel cells, batteries, electrolysis, and many more.[1−6] Nafion is an ideal candidate for a proton exchange membrane but is very expensive. The need of the present time is to develop a low cost, highly conducting, and thermally and mechanically stable polymer electrolyte membrane. PEEK is a fully aromatic polymer having good thermal and mechanical stability and can be easily made hydrophilic by controlled sulfonation from 45% to 65% degree of sulfonation.[7,8] Proton conduction of the SPEEK can be increased by achieving more sulfonation, but it reduces its chemical and mechanical strength.[9] Composite material is the alternative way to improve the properties of the PEM.[10−13]

Carbon nanotubes (CNTs) have emerged as an attractive class of nanomaterial. After their discovery by Ijima, there has been considerable interest in CNT research.[14] A CNT possesses distinct structural dependent electrical, mechanical, and optical properties beneficial for many applications.[15−20] Exploiting these unique physical and mechanical features of CNTs with a polymer matrix leads to the nanocomposites with improved properties. A CNT is used as a reinforcing agent in a polymer matrix. The presence of CNTs within a polymer matrix improves the tensile strength, mechanical properties, and thermal and electrical conductivity.[21−24] However, the low solubility, bad dispersibility, and poor reactivity of CNTs, due to van der Waals forces, limit its processing. For high performance polymer/CNT nanocomposites, proper dispersion and strong interfacial interaction is essential. One of the ways to meet this challenge is the surface modification of CNTs by chemical functionalization, which also prevents CNTs from agglomeration within the polymer matrix. Surface treatment of CNTs with acids such as carboxylic acid and sulfuric acid introduces functional groups onto CNT walls, which help to enhance interaction with the polymer matrix.[25,26]

Again, the orientation of the nanotubes in to the polymer matrix is also a problem that leads to the reduction of performance. Electric and magnetic fields are powerful tools for the proper orientation of CNTs into the base matrix. Alignment of CNTs within the polymer matrix using an electric field has been reported by many authors.[27−29] The high aspect ratio of CNTs makes them highly anisotropic in nature, so it is

Received: September 4, 2014
Accepted: December 16, 2014
Published: December 16, 2014

DOI: 10.1021/am506033c
ACS Appl. Mater. Interfaces 2015, 7, 264−272

Scheme 1. Schematic Representation for Functionalization of CNTs and Their Composite with SPEEK

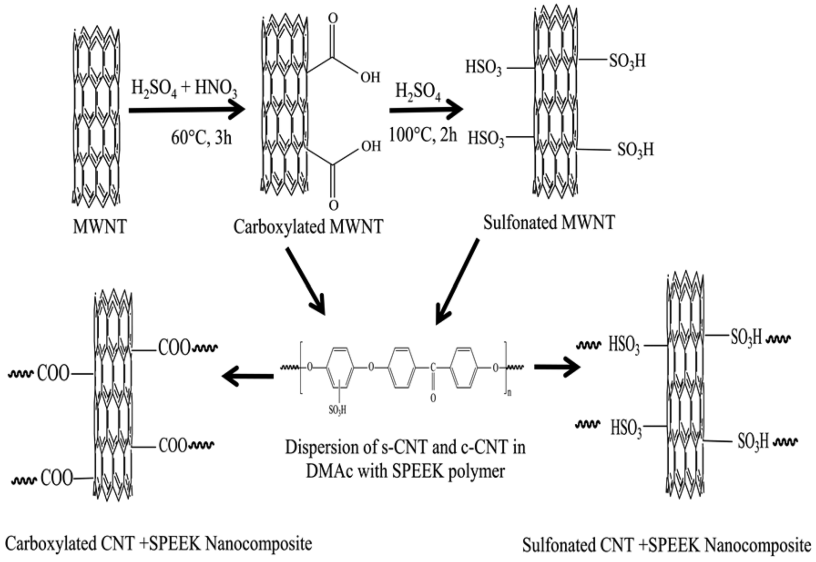

important to have aligned CNTs in the polymer matrix and utilize their anisotropic structure to have improved properties in the direction of alignment. Joo et al. have shown improved mechanical strength in terms of tensile strength, strain, and toughness with a functionalized CNT/sPAS composite membrane.[30] Ma et al. demonstrated the alignment and dispersion of functionalized carbon nanotubes in polymer composites by inducing an electric field.[31] Kumar et al. showed the enhancement of hydrogen gas permeability in electrically aligned MWCNT−PMMA composite membranes.[32]

The present paper describes the preparation of an electrically aligned *f* CNT/SPEEK nanohybrid PEM with varying concentration of *f* CNT (0.1, 0.2. and 0.5%) within a SPEEK matrix. Chemical, structural, thermal, and mechanical characterizations are done using the respective analysis techniques. Membranes were studied extensively by electrochemical and physicochemical properties. Proton conductivity at different temperatures is also measured.

EXPERIMENTAL SECTION

Materials and Methods. Poly ether ether ketone (PEEK) was purchased from Solvay Chemicals. Multiwalled carbon nanotubes (MCNTs) with a diameter of 20−50 nm and length of 5−15 μm were purchased from TCI Chemicals. Other chemicals were obtained commercially and used as received without further purification.

Sulfonation of PEEK was done using conc. H_2SO_4 at 60 °C under constant stirring.[33−35] In brief, 25 g of PEEK powder was dried at 70 °C for 2 h, and then dissolved in 250 mL of conc. H_2SO_4 with constant stirring. After complete dissolution, the solution was heated for 6 h at 55−60 °C with stirring and further stirred for 24 h at room temperature. Then, the polymer solution was gradually precipitated into excess of ice-cold water and washed several times to attain a neutral pH. Sulfonated PEEK (SPEEK) was dried and stored for further use.

Functionalization of the CNTs was done in two steps, first by carboxylic acid treatment and then by sulfonation (Scheme 1). In order to remove the impurities and graft a carboxylic acid functional group on the surface, CNTs were oxidized according to the procedure described elsewhere,[36] where MWCNTs were dispersed in a mixture of sulfuric and nitric acid (1:3 v/v) and heated up to 60 °C with stirring under reflux for 3 h. Subsequently, the nanotubes have been washed with the excess of acid by filtration and dispersion in water, dried, and stored for further use. Carboxylic acid treated CNTs are designated as c-CNT.

Now, c-CNT are further treated with sulfuric acid to add sulfonic acid groups on their walls. Sulfonation of c-CNT was done by dispersing c-CNT in conc. H_2SO_4 and sonicating for 2 h, followed by 2 h heating at 100 °C.[37] Further, the obtained nanotubes are washed with distilled water, filtered, and dried. Obtained CNTs are designated as s-CNT.

For membrane preparation, functionalized CNTs are dispersed in *N*,*N*′-dimethylacetamide (DMAC) by sonication for 2 h. SPEEK is dissolved in dispersed CNT solution and stirred for 5−6 h to get a homogeneous solution, followed by 2 h sonication. The homogeneous solution is poured on a clean glass plate placed between two electrodes of a high voltage power supply. The setup for electric field alignment consists of two electrodes with the separation of 10 cm with 500 V/cm^2 applied potential. In this arrangement, the perpendicular electric field is applied during membrane drying. Alignment of CNTs within the polymer matrix can be explained by the electrophoretic effect.[38] The field is applied throughout the drying process of the membrane. After the membrane is dried, it is peeled off from the glass plate. The membranes are dried at 100 °C in a vacuum oven for 24 h to complete removal of solvent. Membranes of various concentrations of functionalized CNTs (0, 0.1, 0.2, and 0.5 wt %) are prepared and designated as S-cCNT-1, S-cCNT-2, and S-cCNT-5 for carboxylated CNTs and S-sCNT-1, S-sCNT-2, and S-sCNT-5 for sulfonated CNTs, respectively.

Chemical and Structural Characterization. The samples have been characterized by the means of chemical and structural properties by the means of FTIR, SEM, and AFM; details of the characterization are included in the Supporting Information.

Thermal and Mechanical Stability of Membranes. Thermomechanical stabilities of the membrane samples are evaluated by the DMA, TGA, and DSC. Stress/strain curves for hybrid membranes are measured using a Zwick Roell, Z2.5 universal testing machine (UTM). Details of the characterization are included in the Supporting Information.

Physiochemical and Electrochemical Characterization. Water uptake behavior of membranes is determined by recording the weight gain after equilibrating in water for 24 h. Ion-exchange capacity (IEC) of hybrid membranes was estimated by the acid base titration. Proton conductivity of the membranes was measured on a potentiostat/galvanostat (Auto Lab, Model PGSTAT 30). Proton diffusion coefficient for the membranes is calculated using membranes conductivity. Electronic conductivity of the membranes are calculated using *i*−*v* characteristics (−10 to +10 V) using a Keithley electrometer. Details of the experiments are given in the Supporting Information.

DOI: 10.1021/am506033c
ACS Appl. Mater. Interfaces 2015, 7, 264−272

Methanol Permeability Measurements. Methanol permeability of the membranes is carried out in a two-compartment cell in recirculation mode at room temperature. Before performing the experiments, membranes are equilibrated in a feed solution for 12 h. The initial and final concentrations of the solution are measured by using a digital refractometer (Mettler Toledo refractometer). Experimental details are included in the Supporting Information.

RESULT AND DISCUSSION

Structural Characterization of Nanohybrid Membranes. The alignment of *f* CNT in the polymer matrix has been performed by applying a constant electric field of 500 V·cm^{-2}. Because of the difference in the dielectric constant of CNTs and polymer, a dipole moment is induced when an electric field is applied on the CNTs embedded in the polymer. This strong dipole moment in the axis parallel to the length of the nanotubes aligns the CNTs perpendicular to the electrodes and in the direction of the electric field. The schematic representation of electric field aligned *f* CNT/SPEEK preparation is shown is Scheme 2.[39]

Scheme 2. Schematic Representation of Electric Field Aligned CNT/SPEEK Composite Membrane

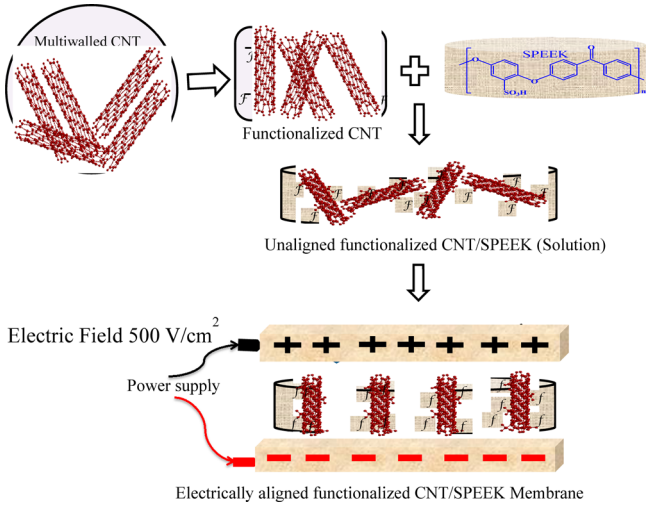

Functionalization of CNTs is done in two ways: First, CNTs are treated with sulfuric and nitric acids to remove impurities and graft carboxylic groups onto their walls. Second, carboxylic acid grafted CNTs (c-CNT) are treated with sulfuric acid to introduce sulfonic acid groups on CNT walls (s-CNT). Figure 1A shows the FTIR spectra of pristine CNT, c-CNT, and s-CNT. Because of the functionalization, different bands have been attached to the CNT walls. The pristine CNT shows a peak at 1518 cm^{-1}, ascribed to the C=C bond. The peaks emerging in c-CNT at 3300–3600, 2329, and 1632 cm^{-1} correspond to O–H bonds from the carboxyl group, O–H stretch from strongly hydrogen bonded –COOH, and C=C.[40,41] For s-CNT, the broad stretching frequency at 3429 cm^{-1} corresponds to the –OH bond, which indicates the existence of COOH and SO_3H groups. The peak emerging at 2921 cm^{-1} in both c-CNT and s-CNT indicates C–H vibration, and the peak at 1630 cm^{-1} may be due interaction between localized C–C bonds and carboxylic acids and ketones.[42,43] Frequencies at 1383 and 1097 cm^{-1} indicate the O–S–O asymmetric and symmetric stretching modes in sulfonated CNTs.

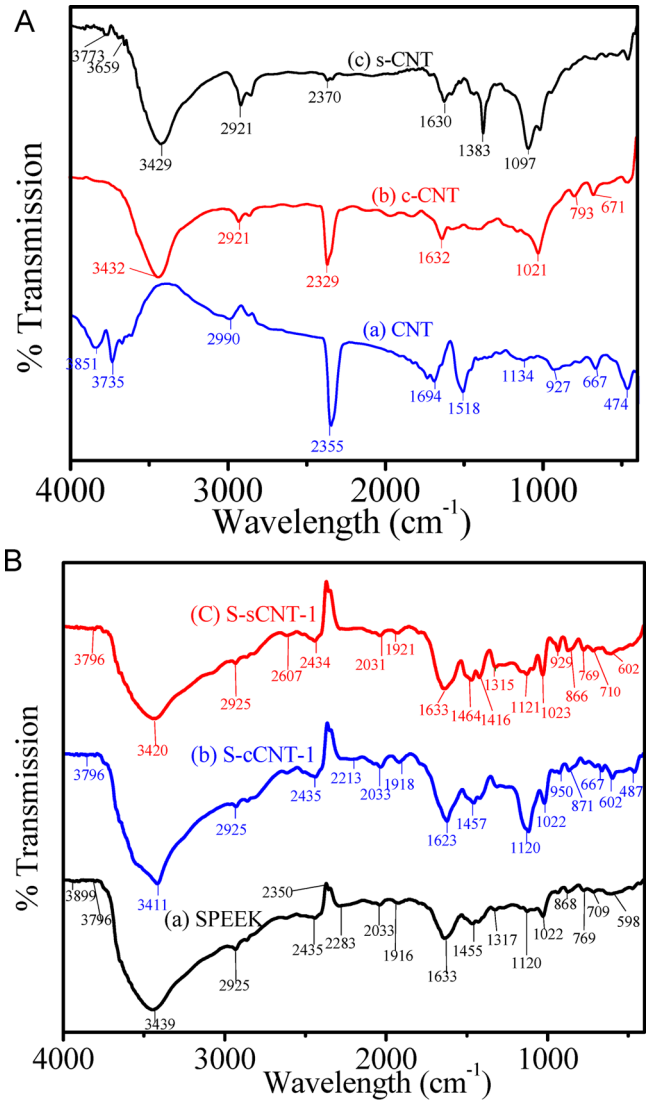

Figure 1. (A) FTIR spectra of CNT, c-CNT, and s-CNT. (B) FTIR spectra of SPEEK, S-cCNT-1, and S-sCNT-1 membranes.

FTIR spectra of SPEEK, S-cCNT-1, and S-sCNT-1 are shown in Figure 1B. The stretching frequency at 3439 cm^{-1} in SPEEK, 3411 cm^{-1} in S-cCNT-1, and 3420 cm^{-1} in S-sCNT-1 indicate O–H vibration (hydrogen bond), while frequencies at 2925 and 2435 cm^{-1}, for SPEEK, S-cCNT-1, and S-sCNT-1, indicate the presence of O–H stretching (acidic group) in membranes. It can be seen that there is a slight peak shift in the *f* CNT/SPEEK membrane compared to the SPEEK membrane, which shows the interaction of *f* CNT to the SPEEK matrix.

The alteration on the sidewall due to the functionalization of CNTs is confirmed by the Raman spectroscopy. Figure 2 and Figure S1 (Supporting Information) show the Raman spectra of functionalized CNTs and SPEEK/*f* CNT membranes, and the corresponding D and G band values are shown in Table S-1 (Supporting Information). In Figure 2, the D band can be observed at 1336 and 1345 cm^{-1} for c-CNT and s-CNT, respectively, which is attributed to the defects or sidewall functionalization of CNTs, while the G band is observed at 1560 and 1581 cm^{-1} for c-CNT and s-CNT, respectively, which can be classified as the tangential stretching mode of graphite.[44–46] Figure S1 demonstrates the Raman spectra of SPEEK/*f* CNT membranes. The D band is observed at 1345

DOI: 10.1021/am506033c
ACS Appl. Mater. Interfaces 2015, 7, 264–272

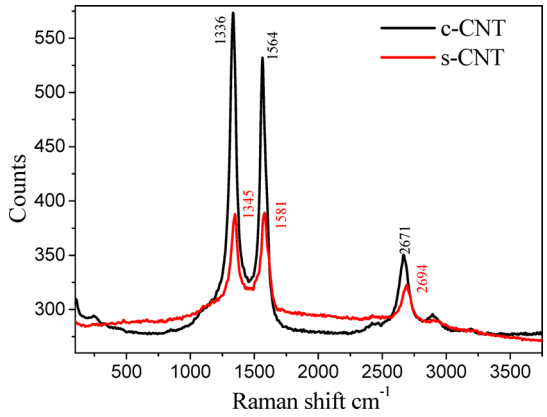

Figure 2. Raman spectra of c-CNT and s-CNT.

and 1320 cm^{-1} for S-cCNT-5 and S-sCNT-5, and the second band, i.e., "G band", was observed at 1574 cm^{-1} for S-cCNT-5 only. The G band also indicates the damage of nanotubes walls after functionalization. G′ peaks observed at ∼2600 cm^{-1} in c-CNT and s-CNT are due to the charge exchanged between carbon nanotubes. The corresponding I_D/I_G values are also illustrated in Table 1 Generally, a lower value of I_D/I_G corresponds to the high purity of the sample.[47] XRD spectra of CNT and S-sCNT-5 are shown in Figure S2 (Supporting Information). The 2θ peak for CNTs at 26.33° well matched with the literature.[48] In the hybrid membrane, the peak of CNT goes diminished and denotes the amorphous nature of the hybrid membrane.

Table 1. Mechanical Properties of Different Nanohybrid PEMs

sample	elastic modulus (MPa)	stress (MPa)	elongation at break (%)
SPEEK	17.42 ± 0.5	92.19 ± 0.8	6.37 ± 0.2
S-sCNT-2	33.98 ± 0.5	127.27 ± 0.8	20.04 ± 0.2
S-sCNT-5	16.13 ± 0.5	54.59 ± 0.8	9.15 ± 0.2

Surface and cross-sectional images of *f* CNT/SPEEK membranes are shown in Figure 3. The cross-sectional view of S-cCNT-5 and S-sCNT-5 shows the distribution of *f* CNT in SPEEK (Figure 3B,C). It is clear from the figure that the distribution of *f* CNT in the SPEEK matrix is uniform, which is also confirmed by the AFM images of SPEEK, cCNT-5, and S-sCNT-5. Surface roughness of the membranes is also calculated by AFM images, which are found to be in increasing order by introducing the *f* CNT in the SPEEK matrix. TEM images of randomly and aligned *f* CNT membranes are shown in Figure 4. The figure demonstrates the unaligned and aligned *f* CNT within the SPEEK polymer matrix. Alignment can be clearly seen in Figure 4B,C, while Figure 4A shows the unaligned CNTs in the polymer matrix.

Thermal and Mechanical Properties of Nanohybrid Membrane. TGA of CNT and electrically aligned *f* CNT/SPEEK membranes is performed to analyze the thermal stability of the samples. Figure 5 and Figure S3 (Supporting Information) shows the TGA and DTG thermographs for CNT, c-CNT, and s-CNT. It can be seen from the figure that CNT is more stable than the *f* CNT up to 600 °C since there is only 2.5% weight loss in CNT while 8.4% and 13.1% weight loss is observed in c-CNT and s-CNT, respectively. Two weight loss steps are found in CNTs: one is at around 100 ° C due to the presence of moisture, and another is between 260 and 310 °C observed due to the degradation of functional groups present in the CNT. The amounts of the carboxylate and sulfonate moiety of the *f* CNT are determined using a weight loss difference between virgin CNT and *f* CNT at 600 °C.[49] It was found that the presence of about 5.9 wt % carboxylate and 10.6 wt % sulfonate content in *f* CNT indicates that the method applied in this work is effective for functionalization of CNTs. TGA and DTG thermographs for nanohybrid membranes are depicted in Figure 6 and Figure S4 (Supporting Information). Three weight loss steps could be observed in the corresponding TGA curves of hybrid membranes. The observed weight losses are between the ranges of 50−150 °C, 250−400 °C, and 450−600 °C for S-cCNT membranes. For S-sCNT membranes, the observed weight losses are from 40−10 °C, 280−430 °C, and 480−570 °C. The first weight loss is attributed to the evaporation of hydrated water present in the membranes; the second is assigned to the decomposition of carboxylic and sulfonic acid groups present in the CNT and SPEEK matrix, while the last weight loss around 500 °C is due to the decomposition of the polymer backbone. The hybrid membranes shows the higher degradation temperature than the pristine SPEEK membrane. Also, the S-sCNT membrane

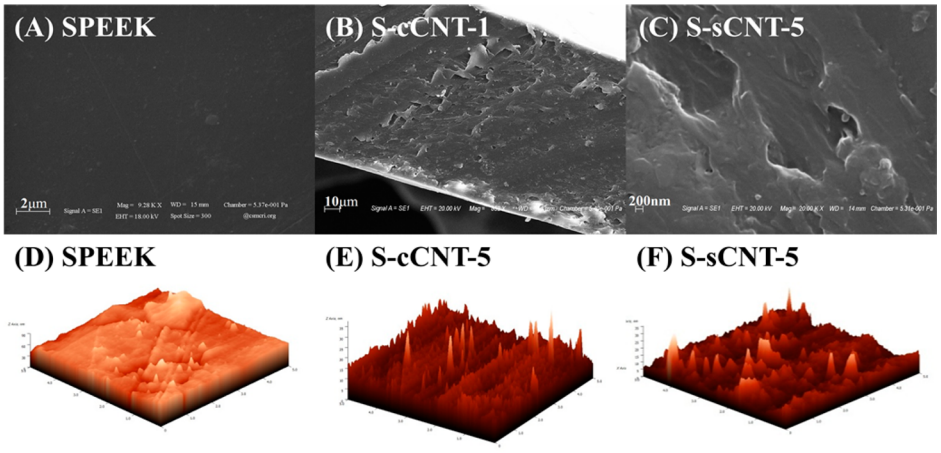

Figure 3. SEM (A, B, C) of SPEEK, S-cCNT-1, S-sCNT-5; and AFM (D, E, F) of SPEEK, S-cCNT-5, S-sCNT-5 of SPEEK/*f* CNT composite membranes.

DOI: 10.1021/am506033c
ACS Appl. Mater. Interfaces 2015, 7, 264−272

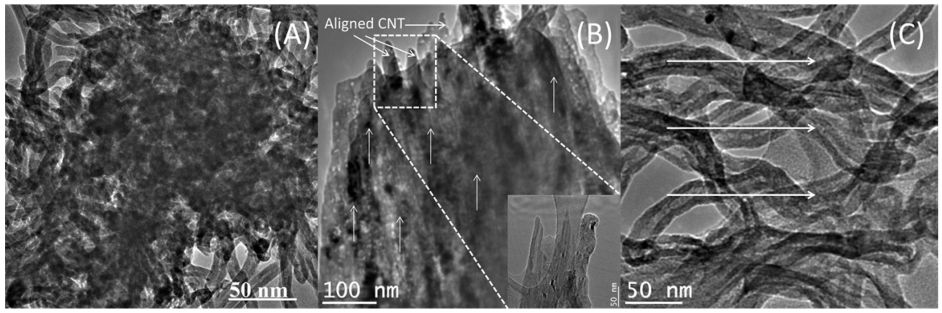

Figure 4. TEM of (A) randomly distributed, (B, C) electrically aligned SPEEK/*f* CNT (S-sCNT-5) composite membranes (arrows show the direction of CNT alignment).

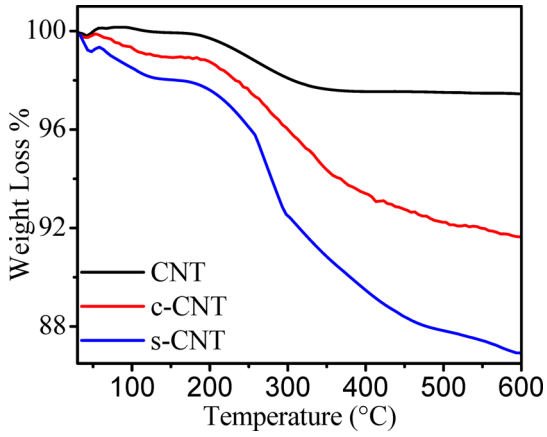

Figure 5. TGA thermographs for CNT, c-CNT, and s-CNT.

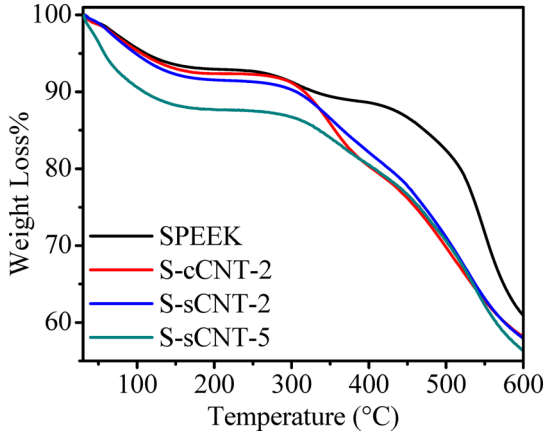

Figure 6. TGA thermographs for SPEEK, S-cCNT-2, S-sCNT-2, and S-sCNT-5 membranes.

reveals a higher degradation temperature than the S-cCNT membrane, due to the better interaction between s-CNT and SPEEK compared to c-CNT and SPEEK. DSC curves for the hybrid membranes are shown in Figure S5 (Supporting Information). A single crystalline peak is observed for SPEEK and *f* CNT/SPEEK hybrid membranes, showing the better interaction between *f* CNT and SPEEK, as confirmed by the TGA analysis.

DTMA analysis shows the thermo-mechanical stability of the membranes (Figure 7). The storage modulus increased with the increase in s-CNT concentration within the SPEEK matrix. The highest value of modulus was found to be at 2503 MPa for the S-sCNT-5 membrane, which is almost 2.4 times higher than

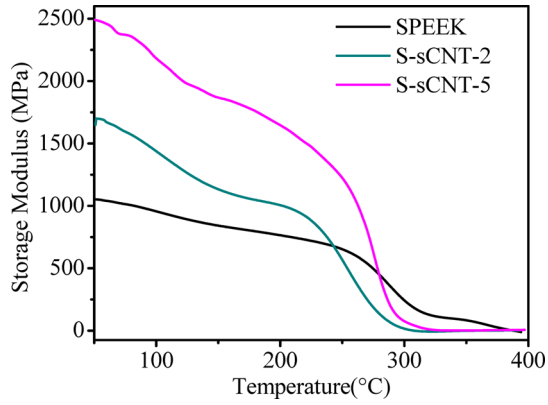

Figure 7. DMA of SPEEK, S-sCNT-2, and S-sCNT-5 membranes.

that for the SPEEK membrane. The enhancement in the storage modulus of S-sCNT membranes indicates the strong bonding due to the presence of a common sulfonic acid group in CNT and PEEK, and the effect of electric field for the alignment of CNTs in the SPEEK matrix. Furthermore, alignment of CNTs using an electric field makes them more oriented, which restricts the movement of the polymer chains and which further increases the stiffness of the polymer. The tan δ value is also found to be increased by 20% in the S-sCNT-5 membrane than the SPEEK membrane. The stress–strain curves for the membranes are shown in Figure 8, and the calculated values for elastic modulus, stress, and maximum elongation are presented in Table 1. The S-sCNT-2 membrane shows the maximum value for elastic modulus, which is almost

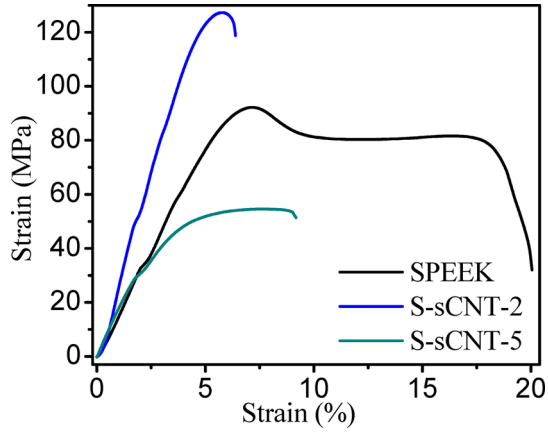

Figure 8. Stress/strain curves for SPEEK, S-sCNT-2, and S-sCNT-5 membranes.

DOI: 10.1021/am506033c
ACS Appl. Mater. Interfaces 2015, 7, 264–272

Table 2. Ion-Exchange Capacity, Water Uptake (%), Number of Water Molecules Per Ionic Site (λ), Free and Bound Water (%), and Dimensional Change (%) for Different Nanohybrid PEMs

membrane type	IEC (meq·gm^{-1})	water uptake (%)	λ (SO_3/H_2O)	free water (%)	bound water (%)	dimensional change (%)
SPEEK	1.59 ± 0.05	26.02 ± 1.0	9.09 ± 0.2	25.43 ± 1.8	0.59 ± 0.2	19.54 ± 0.5
S-cCNT-2	1.89 ± 0.05	32.90 ± 1.0	9.67 ± 0.2	32.12 ± 1.8	0.78 ± 0.2	16.18 ± 0.5
S-sCNT-1	1.91 ± 0.05	37.02 ± 1.0	10.82 ± 0.2	35.95 ± 1.8	1.07 ± 0.2	18.52 ± 0.5
S-sCNT-2	2.12 ± 0.05	41.8 ± 1.0	10.95 ± 0.2	40.64 ± 1.8	1.16 ± 0.2	16.55 ± 0.5
S-sCNT-5	2.19 ± 0.05	43.85 ± 1.0	11.10 ± 0.2	42.67 ± 1.8	1.18 ± 0.2	11.80 ± 0.5
Nafion 117	0.9 ± 0.05	23.02 ± 1.0	8.0 ± 0.2			

Table 3. Membrane Ionic Conductivity (σ), Membrane Electronic Conductivity ($\sigma_{(E)}$), Diffusion Coefficient (D_σ), Methanol Permeability (P_m), Selectivity (S), and Activation Energy of Proton Conduction (E_a) of Different Nanohybrid PEMs

membrane type	σ ($\times 10^{-2}$) (S·cm^{-1})	$\sigma_{(E)}$ (S·cm^{-1})	D_σ ($\times 10^{-10}$) (m^2 S^{-1})	P_m ($\times 10^{-7}$) (cm^2 s^{-1})	S ($\times 10^5$)	E_a (kJ mol^{-1})
SPEEK	2.01 ± 0.01	2.50×10^{-5}	1.251 ± 0.05	2.107 ± 0.1	0.95 ± 0.1	23.18 ± 0.5
S-cCNT-2	2.35 ± 0.01	5.53×10^{-3}	1.582 ± 0.05	1.961 ± 0.1	2.39 ± 0.1	19.82 ± 0.5
S-sCNT-1	3.57 ± 0.01	2.54×10^{-3}	1.701 ± 0.05	1.723 ± 0.1	4.14 ± 0.1	16.24 ± 0.5
S-sCNT-2	3.77 ± 0.01	7.10×10^{-3}	2. 413 ± 0.05	1.701 ± 0.1	4.45 ± 0.1	15.32 ± 0.5
S-sCNT-5	4.31 ± 0.01	7.66×10^{-3}	2.732 ± 0.05	1.689 ± 0.1	5.10 ± 0.1	13.69 ± 0.5

double that of the SPEEK membrane, while the maximum stress is found for the SPEEK membrane. All the hybrid membranes are stable mechanically and thermally and can be used for the high temperature applications.

Ion-Exchange Capacity, Water Retention Capability, and Dimension Stability of Nanohybrid PEMs. The key properties of nanohybrid PEMs, including IEC, water uptake, hydration number, and dimensional stability, are presented in Table 2. The IEC is an important parameter of PEMs, which is affected by the density of functional groups present in the polymer matrix. In present case, IEC of prepared membranes increases as the concentration of aligned CNTs increases for both S-cCNT and S-sCNT membranes. The IEC of S-sCNT-2 membranes is around 11% higher than those of S-cCNT-2 membranes, resulting from the higher content of sulfonic groups in CNTs compared to carboxylic group content in CNTs, confirmed by TGA of CNTs. In proton conducting membranes, water uptake is an important parameter as it directly affects the transportation properties and is related to the IEC of the membranes. The high value of IEC displays a higher water uptake in the membrane. It is evident from water uptake measurements that the value increases with CNT content in membranes. SPEEK shows 26% water uptake, while it increases for the S-cCNT membrane, which is 32.9%. For the S-sCNT membrane, the water uptake further increases and reaches to 43.85% for S-sCNT-5; the water uptake for S-sCNT-5 is about 68% higher than that for SPEEK due to its higher IEC and the presence of aligned CNTs in the matrix. Water molecules per unit functional group (λ) for the hybrid membranes are calculated by the following equation:

$$\lambda = \left(\frac{\text{Water uptake}}{18.01}\right)\left(\frac{10}{\text{IEC}}\right)$$

The water content (λ) value for SPEEK is found to be 9.1, which goes to increases by 11.1 for the S-sCNT-5 membrane. The increment in λ is due to the corresponding ion-exchange capacity of SPEEK; the IEC for S-sCNT-5 is found to be 36.7% higher than that for the SPEEK membrane due to the presence of highly acidic functionalized sCNT, as shown in Table 2. It is clear from the results that, by increasing the sCNT content, the water molecules surrounding SO_3H increases from 9.1 to 11.1. Unfortunately, the higher water uptake reduces the dimensional and mechanical stability, but no reduction is found in the case of S-sCNT membranes. Dimensional change reduces by 40% from SPEEK to S-sCNT-5; it may be due to the interaction of sCNTs with the SPEEK matrix as SPEEK is confined between adjacent nanotubes, which hinders swelling of the membranes.[50,51] There exist two types of water, bound and free inside PEM. For the conduction of protons, bound water is more responsible than free water, which is calculated by TGA analysis from 100 to 150 °C, while free water is the difference of water content to the bound water present in membrane. SPEEK membranes show the lowest bound water content (0.59%) in comparison with all membranes (Table 2), while 1.18% bound water in the S-sCNT-5 membrane, maintains the high water retention ability.

Proton Conductivity and Diffusion Coefficient Measurements. Integrating the high surface functionalized aligned CNTs in a polymer matrix improves the IEC, water uptake and thus enhances the proton conductivity and transport through the membranes. The proton conductivity of the membrane is significantly improved due to three main effects of the additives: the additional hydrophilic sulfonic acid groups supported by the high surface area of CNTs, the inherent property of carbon material to retain both the physical and the chemically bound moisture, and the creation of pores by the vertically alligned CNTs into the SPEEK matrix, creating free volume to absorb more water. Since the immigration of H_3O^+ ions is encouraged by the water channels, the conductivity of the membrane increased, following the same fashion of the IEC as well as water uptake. Proton conductivity of the S-sCNT-5 membrane reaches 4.31×10^{-2} S·cm^{-1}, which is more than twice that of the SPEEK membrane (Table 3). This is due to the presence of more sulfonic groups within the matrix, which provide the ion conducting path for the movement of ions. For the high temperature applications, the temperature dependent proton conductivity of PEMs are measured from 30 to 90 °C, as presented in Figure 9. It can be seen from the figure that, as the temperature increases, the proton conductivity of PEMs increases, and the value of proton conductivity for S-sCNT-5 reaches to 12.41×10^{-2} S·cm^{-1} from its initial value of 4.31×10^{-2} S·cm^{-1}, which is equivalent to the nafion membrane. Conductivity for all the membranes was found to be improved by 2.6−3.0 times by increasing the temperature from 30 to 90

DOI: 10.1021/am506033c
ACS Appl. Mater. Interfaces 2015, 7, 264−272

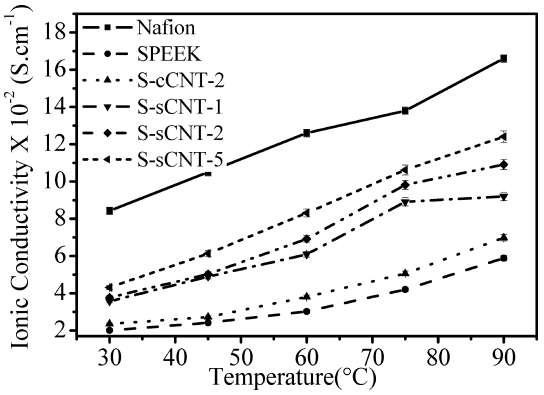

Figure 9. Plot of ionic conductivity vs temperature for different membranes.

°C, which may be due to the increment in proton diffusion with temperature.[52] The dependence of proton diffusion coefficient on *f* CNT content is evaluated using membrane conductivity.[53] Table 3 shows the calculated values of diffusion coefficient (D_σ) for different PEMs, displaying the increased D_σ value by increasing the S-sCNT content in the SPEEK matrix. This indicates that the incorporation of *f* CNT can increase the applicability of the SPEEK membranes not only for room temperature but also for high temperature applications. Activation energy for proton transport for one functional group to another is calculated by the Arrhenius-type plot, as shown in Figure S6 (Supporting Information) and Table 3. It is clear from the table that the activation energy required for the migration of ions is reducing by incorporation of *f* CNT content in the SPEEK matrix, and required lower energy for the S-sCNT-5 membrane.

Current−Voltage (*i*−*v*) Characteristics of Hybrid Membranes. Current−voltage (*i*−*v*) characteristics of SPEEK, S-sCNT-2 (without field), and S-sCNT-2 (with field) are shown in Figure 10A. *i*−*v* measurements are performed using a four-probe system. There is a dramatic change in *i*−*v* characteristics of the electrically aligned S-sCNT-2 PEM as compared to the randomly oriented S-sCNT-2 (without field) and pristine SPEEK membrane. SPEEK and S-sCNT-2 (without field) membranes show almost negligible current compared to the electrically aligned S-sCNT-2 membrane. While the increased trend in current in the aligned S-sCNT-2 membrane can be explained as, when electric field is applied, then CNT forms the conducting channel between the electrodes and established the Ohmic contact between the electrode and the PEM. In the randomly oriented S-sCNT-2 (without field) PEM, CNTs within the polymer matrix do not carry any current and do not provide any conducting path for current flow.[32] Furthermore, the current enhances with applied potential as the concentration of CNTs increases within the polymer matrix. It can be seen from Table 3 that the maximum conductivity is obtained for S-sCNT-2 for both c-CNT and s-CNT membranes. The S-sCNT-5 (aligned) membrane shows less electronic conductivity, which may be due to the agglomeration of CNTs, hindering the conduction of electrons. The total tunneling current has a kink that is a function of the applied potential. From Figure 10B,C, it can be seen that the kink becomes a step in the differential conductance (dI/dV) plot and a peak in the d^2I/dV^2 plot.[54] The nonlinearity of *i*−*v* curves indicates the semiconducting behavior of aligned CNTs

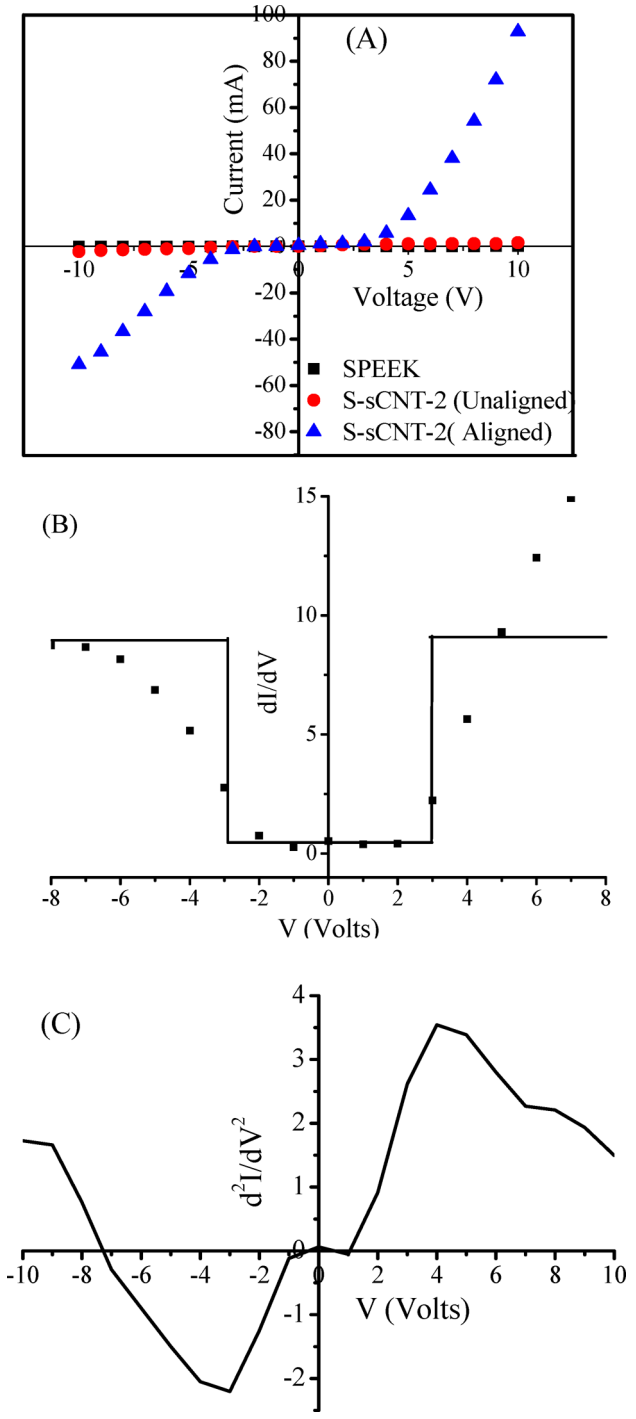

Figure 10. Current−voltage (*i*−*v*) characteristics for SPEEK/CNT composites (A), corresponding voltage (*V*) versus dI/dV (B), and voltage (*V*) versus d^2I/dV^2 (C) plots.

and their ability to be used for the fabrication of nanoelectrode materials.

Methanol Permeation (P_m) Resistance and Selectivity of Nanohybrid Membranes. For DMFC application, the PEM should have high proton conductivity with low methanol permeation. Methanol permeability of SPEEK and S-sCNT PEMs is shown in Table 3. It is clear from the results that the methanol permeability of S-sCNT PEMs decreased with increment of CNT content in SPEEK. In the case of S-sCNT PEMs, CNTs prevent the movement of methanol through the

DOI: 10.1021/am506033c
ACS Appl. Mater. Interfaces 2015, 7, 264−272

membrane and act as barriers for connected hydrophilic channels as well as provide the higher conductivity to the hybrid membrane. The interaction between *f* CNT and SPEEK restricts the formation of free volume in membranes, which leads to low methanol permeability. Methanol permeability for the SPEEK membrane is found to be 2.107×10^{-7} cm^2 S^{-1}, which reduces to 1.961×10^{-7} cm^2 s^{-1} for the S-cCNT-2 membrane and 1.701×10^{-7} cm^2 s^{-1} for S-sCNT-2 membranes and finally reached to 1.689×10^{-7} cm^2 s^{-1} for the S-sCNT-5 membrane. Reduction in methanol permeability for S-sCNT PEMs is due to strong interfacial adhesion between *f* CNT and the SPEEK matrix.[42] Selectivity of the membrane, which is directly proportional to the membrane conductivity and inversely proportional to the methanol permeability, is also calculated for PEMs, which is found to be 0.95×10^5 for the SPEEK membrane. The selectivity value for hybrid membranes increases and reaches to 5.1×10^5 for the S-sCNT-5 membrane (Table 3). The low methanol permeability with high selectivity and proton conductivity of S-sCNT-5 PEM makes it suitable for the DMFC application.

CONCLUSION

Electrically aligned *f* CNT/SPEEK nanohybrid PEMs are successfully prepared by a solution casting method. Nanohybrid PEMs with electrically aligned *f* CNT show better performance as compared to randomly aligned *f* CNT. Further, among the prepared membranes, the S-sCNT-5 membrane demonstrates the best performance in comparison to other PEMs. While IEC, conductivity, methanol permeation resistance and selectivity of the membranes are enhanced, the membrane still maintained excellent thermal and mechanical stability. All the membranes show the good proton conductivity at higher temperatures and have reduced activation energy for proton conduction by addition of *f* CNT. The dramatic enhancement in current in S-sCNT membranes indicates that aligning the *f* CNT within SPEEK greatly affects the properties and performance of the PEM membrane in a better way. The good exhaustive affairs and stability make the *f* CNT/SPEEK nanohybrid membranes a swatch candidate for fuel cell membranes and electrodes up to a high temperature range.

ASSOCIATED CONTENT

Supporting Information

The details of the chemical, structural, and physiochemical characterization and membranes stability are included in the Supporting Information. Figures S1−S6 are also included. This material is available free of charge via the Internet at http://pubs.acs.org.

AUTHOR INFORMATION

Corresponding Author

*E-mail: vaibhavk@csmcri.org, vaibhavphy@gmail.com. Tel: +91-278-2567039. Fax: +91-278-2567562 (V.K.).

Notes

The authors declare no competing financial interest.

ACKNOWLEDGMENTS

V.K. is thankful to the Department of Science and Technology, New Delhi, for providing financial support. Financial support received from CSIR Network projects (CSC 0105 and CSC 0115) is also acknowledged. The authors are also thankful to the Analytical Discipline and Centralized Instrument facility, CSMCRI, Bhavnagar, for instrumental support.

REFERENCES

(1) Gahlot, S.; Sharma, P. P.; Kulshrestha, V.; Jha, P. K. SGO/SPES-Based Highly Conducting Polymer Electrolyte Membranes for Fuel Cell Application. *ACS Appl. Mater. Interfaces* **2014**, *6*, 5595−5601.

(2) Gahlot, S.; Sharma, P. P.; Gupta, H.; Kulshrestha, V.; Jha, P. K. Preparation of Graphene Oxide Nano-composite Ion-Exchange Membranes for Desalination Application. *RSC Adv.* **2014**, *4*, 24662−24670.

(3) Yang, M.; Hou, J. Membranes in Lithium Ion Batteries. *Membranes* **2012**, *2*, 367−383.

(4) Zhang, S. S.; Xu, K.; Jow, R. An Inorganic Composite Membrane as the Separator of Li-Ion Batteries. *J. Power Sources* **2005**, *140*, 361−364.

(5) Song, M. K.; Li, H.; Li, J.; Zhao, D.; Wang, J.; Liu, M. Tetrazole-based, Anhydrous Proton Exchange Membranes for Fuel Cells. *Adv. Mater.* **2014**, *26*, 1277−1282.

(6) Ayyarua, S.; Dharmalingam, S. Improved Performance of Microbial Fuel Cells Using Sulfonated Polyether Ether Ketone (SPEEK) TiO_2-SO_3H Nanocomposite Membrane. *RSC Adv.* **2013**, *3*, 25243−25251.

(7) Mondal, A. N.; Tripathi, B. P.; Shahi, V. K. Highly Stable Aprotic Ionic-Liquid Doped Anhydrous Proton-Conducting Polymer Electrolyte Membrane for High-Temperature Applications. *J. Mater. Chem.* **2011**, *21*, 4117−4124.

(8) Silva, V. S.; Ruffmann, B.; Vetter, S.; Mendes, A.; Madeira, L. M.; Nunes, S. P. Characterization and Application of Composite Membranes in DMFC. *Catal. Today.* **2005**, *104*, 205−212.

(9) Robertson, G. P.; Mikhailenko, S. D.; Wang, K.; Xing, P.; Guiver, M. D.; Kaliaguine, S. Casting Solvent Interactions with Sulfonated Poly(Ether Ether Ketone) During Proton Exchange Membrane Fabrication. *J. Membr. Sci.* **2003**, *219*, 113−121.

(10) Xiao, S. Y.; Yang, Y. Q.; Li, M. X.; Wang, F. X.; Chang, Z.; Wu, Y. P.; Liu, X. A Composite Membrane Based on a Biocompatible Cellulose as a Host Gel Polymer Electrolyte for Lithium Ion Batteries. *J. Power Sources* **2014**, *270*, 53−58.

(11) Harvat, C. I.; Zhu, X.; Trup, D.; Vinokur, R. A.; Demco, D. E.; Fechete, R.; Conradi, O.; Graichen, A.; Anokhin, D.; Ivanov, D. A.; Möller, M. Perfluorosulfonic Acid Ionomer-Silica Composite Membranes Prepared Using Hyperbranched Polyethoxysiloxane for Polymer Electrolyte Membrane Fuel Cells. *Int. J. Hydrogen Energy* **2012**, *37*, 14454−14462.

(12) Xu, Q.; Kong, Q.; Liu, Z.; Wang, X.; Liu, R.; Zhang, J.; Yue, L.; Duan, Y.; Cui, G. Cellulose/Polysulfonamide Composite Membrane as a High Performance Lithium Ion Battery Separator. *ACS Sustainable Chem. Eng.* **2014**, *2*, 194−199.

(13) Sambasivarao, S. V. Thermal Stability and Ionic conductivity of High-Temperature Proton Conducting Ionic Liquid Polymer Composite Electrolyte Membranes for Fuel Cell Applications, Polymer Composites for Energy Harvesting, Conversion, and Storage. *ACS Symp. Ser.* **2014**, *1161*, 111−126.

(14) Iijima, S. Helical Microtubules of Graphitic Carbon. *Nature* **1991**, *354*, 56−58.

(15) O'Connell, M. J.; Bachilo, S. M.; Huffman, C. B.; Moore, V. C.; Strano, M. S.; Haroz, E. H.; Rialon, K. L.; Boul, P. J.; Noon, W. H.; Kittrell, C.; Ma, J.; Hauge, R. H.; Weisman, R. B.; Smalley, R. E. Band Gap Fluoresnence from Individual Single-Walled Carbon Nanotubes. *Science* **2002**, *297*, 593−596.

(16) Prehn, K.; Adelung, R.; Heinen, M.; Nunes, S. P.; Schulte, K. Catalytically Active CNT−Polymer-Membrane Assemblies: From Synthesis to Application. *J. Membr. Sci.* **2008**, *321*, 123−130.

(17) Moulton, S. E.; Minett, A. I.; Wallace, G. G. Carbom Nanotube Based Elecronic and Electrochemical Sensors. *Sens. Lett.* **2005**, *3*, 183−193.

(18) Terrones, M. Carbon Nanotubes: Synthesis and Properties, Electronic Devices and Other Emerging Applications. *Int. Mater. Rev.* **2004**, *49*, 325−377.

DOI: 10.1021/am506033c
ACS Appl. Mater. Interfaces 2015, 7, 264−272

(19) Tasis, D.; Tagmatarchis, N.; Bianco, A.; Prato, M. Chemistry of Carbon Nanotubes. *Chem. Rev.* **2006**, *106*, 1105−1136.
(20) Graham, A. P.; Duesberg, G. S.; Seidel, R. V.; Liebau, M.; Unger, E.; Pamler, W.; Kreupl, F.; Hoenlein, W. Carbon Nanotubes for Microelectronics? *Small* **2005**, *1*, 382−390.
(21) Andrews, R.; Weisenberger, M. C. Carbon Nanotube Polymer Composites. *Curr. Opin. Solid State Mater. Sci.* **2004**, *8*, 31−37.
(22) Jin, S. H.; Park, Y. B.; Yoon, K. H. Rheological and Mechanical Properties of Surface Modified Multi-Walled Carbon Nanotube-Filled PET Composite. *Compos. Sci. Technol.* **2007**, *67*, 3434−3441.
(23) Singh, I. V.; Tanaka, M.; Zhang, J.; Endo, M. Evaluation of Effective Thermal Conductivity of CNT-Based Nano-Composites by Element Free Galerkin Method. *Int. J. Numer. Methods Heat Fluid Flow* **2007**, *17*, 757−769.
(24) Grossiord, N.; Miltner, H. E.; Loos, J.; Meuldijk, J.; Van Mele, B.; Koning, C. E. On the Crucial Role of Wetting in the Preparation of Conductive Polystyrene-Carbon Nanotube Composites. *Chem. Mater.* **2007**, *19*, 3787−3792.
(25) Sahoo, N. G.; Rana, S.; Cho, J. W.; Li, L.; Chan, S. H. Polymer Nanocomposites Based on Functionalized Carbon Nanotubes. *Prog. Polym. Sci.* **2010**, *35*, 837−867.
(26) Flavin, K.; Kopf, I.; Canto, E. D.; Navio, C.; Bittencourt, C.; Giordani, S. Controlled Carboxylic Acid Introduction: A Route to Highly Purified Oxidized Single-Walled Carbon Nanotubes. *J. Mater. Chem.* **2011**, *21*, 17881−17887.
(27) Sharma, A.; Vijay, Y. K. Effect of Electric Field Variation in Alignment of SWNT/PC Nanocomposites. *Int. J. Hydrogen Energy* **2012**, *37*, 3945−3948.
(28) Martina, C. A.; Sandler, J. K.W.; Windle, A. H.; Schwarz, M. K.; Bauhofer, W.; Schulte, K. Electric Field-Induced Aligned Multi-Wall Carbon Nanotube Networks in Epoxy Composites. *Polymer* **2005**, *46* (3), 877−886.
(29) Kim, S.; Fornasiero, F.; Park, H. G.; In, J. B.; Meshot, E.; Giraldo, G.; Stadermann, M.; Fireman, M.; Shan, J.; Grigoropoulos, C. P.; Bakajin, O. Fabrication of Flexible, Aligned Carbon Nanotube/Polymer Composite Membranes by in-Situ Polymerization. *J. Membr. Sci.* **2014**, *460*, 91−98.
(30) Joo, S. H.; Pak, C.; Kim, E. H.; Lee, Y. H.; Chang, H.; Seung, D.; Choi, Y. S.; Park, J. B.; Kim, T. K. Functionalized Carbon Nanotube-Poly(Arylene Sulfone) Composite Membranes for Direct Methanol Fuel Cells with Enhanced Performance. *J. Power Sources* **2008**, *180*, 63−70.
(31) Ma, C.; Zhang, W.; Zhu, Y.; Ji, L.; Zhang, R.; Koratkar, N.; Liang, J. Alignment and Dispersion of Functionalized Carbon Nanotubes in Polymer Composites Induced by an Electric Field. *Carbon* **2008**, *46*, 706−720.
(32) Kumar, S.; Sharma, A.; Tripathi, B.; Srivastava, S.; Agrawal, S.; Singh, M.; Awasthi, K.; Vijay, Y. K. Enhancement of Hydrogen Gas Permeability in Electrically Aligned MWCNT-PMMA Composite Membranes. *Micron* **2010**, *41*, 909−914.
(33) Xing, P.; Robertson, G. P.; Guiver, M. D.; Mikhailenko, S. D.; Wang, K.; Kaliaguine, S. Synthesis and Caracterization of Sulfonated Poly(ether ether ketone) for Proton Exchange Membranes. *J. Membr. Sci.* **2004**, *229*, 96−106.
(34) Zaidi, S. M. J.; Mikhailenko, S. D.; Robertson, G. P.; Guiver, M. D.; Kaliaguine, S. Proton Conducting Composite Membranes from Polyether Ether Ketone and Heteropolyacids for Fuel Cell Applications. *J. Membr. Sci.* **2000**, *173*, 17−34.
(35) Nagarale, R. K.; Gohil, G. S.; Shahi, V. K. Sulfonated Poly(ether ether ketone)/Polyaniline Composite Proton-Exchange Membrane. *J. Membr. Sci.* **2006**, *280*, 389−396.
(36) Firkowska, I.; Boden, A.; Vogt, A. M.; Reich, S. Effect of Carbon Nanotube Surface Modification on Thermal Properties of Copper−CNT Composites. *J. Mater. Chem.* **2011**, *21*, 17541−17546.
(37) Zhou, W.; Xiao, J.; Chen, Y.; Zeng, R.; Xiao, S.; Nie, H.; Li, F.; Song, C. Sulfonated Carbon Nanotubes/Sulfonated Poly(ether sulfone ether ketone ketone) Composites for Polymer Electrolyte Membranes. *Polym. Adv. Technol.* **2011**, *22*, 1747−1752.
(38) Park, C.; Wilkinson, J.; Banda, S.; Ounaies, Z.; Wise, K. E.; Sauti, G. Aligned Single-Wall Carbon Nanotube Polymer Composites Using an Electric Field. *J. Polym. Sci., Part B: Polym. Phys.* **2006**, *44*, 1751−1762.
(39) Stephan, C.; Nguyen, T. P.; Lamy de la Chapelle, M.; Lefrant, S.; Journet, C.; Bernier, P. Characterization of Single Walled Carbon Nanotubes-PMMA Composites. *Synth. Met.* **2000**, *108*, 139−149.
(40) Sepahvand, R.; Adeli, M.; Astinchap, B.; Kabiri, R. New Nanocomposites Containing Metal Nanoparticles, Carbon Nanotube and Polymer. *J. Nanopart. Res.* **2008**, *10*, 1309−1318.
(41) Yang, S.; Li, J.; Shao, D.; Hu, J.; Wang, X. Adsorption of Ni(II) on Oxidized Multiwalled Carbon Nanotubes: Effect of Contact Time, pH, Foreign Ions and PAA. *J. Hazard. Mater.* **2009**, *166*, 109−116.
(42) Peng, F.; Zhang, L.; Wang, H. J.; Lv, P.; Yu, H. Sulfonated Carbon Nanotubes as a Strong Protonic Acid Catalyst. *Carbon* **2005**, *43*, 2405−2408.
(43) Kim, U. J.; Furtado, C. A.; Liu, X. M.; Chen, G. G.; Eklund, P. C. Raman and IR Spectroscopy of Chemically Processed Single-Walled Carbon Nanotubes. *J. Am. Chem. Soc.* **2005**, *127*, 15437−15445.
(44) Hirsc, A. Functionalization of Single-Walled Carbon Nanotubes. *Angew. Chem., Int. Ed.* **2002**, *41*, 853−859.
(45) Hamon, M. A.; Hu, H.; Bhowmik, P.; Niyogi, S.; Itkis, M. E.; Haddon, R. C. End-Group and Defect Analysis of Soluble Single-Walled Carbon Nanotubes. *Chem. Phys. Lett.* **2001**, *347*, 8−12.
(46) Dresselhaus, M. S.; Dresselhaus, G.; Saito, R.; Jorio, A. Raman Spectroscopy of Carbon Nanotubes. *Phys. Rep.* **2005**, *409*, 47−99.
(47) Ghosh, S.; Bachilo, S. M.; Simonette, R. A.; Beckingham, K. M.; Weisman, R. B. Oxygen Doping Modified Near-Infrared Band Gaps in Fluorescent Single-Walled Carbon Nanotubes. *Science* **2010**, *330*, 1656−1659.
(48) Laing, C.; Ding, L.; Li, C.; Pang, M.; Su, D.; Li, W.; Wang, Y. Nanostructured WC_x/CNTs as Highly Efficient Support of Electrocatalysts with Low Pt Loading for Oxygen Reduction Reaction. *Energy Environ. Sci.* **2010**, *3*, 1121−1127.
(49) Zoo, S. H.; Pak, C.; Kim, E. A.; Lee, Y. H.; Chang, H.; Seung, D.; Choi, Y. S.; Park, J. B.; Kim, T. K. Functionalized Carbon Nanotube-Poly(arylene sulfone) Composite Membranes for Direct Methanol Fuel Cells with Enhanced Performance. *J. Power Sources* **2008**, *180*, 63−70.
(50) Chakrabarty, T.; Rajesh, A. M.; Jasti, A.; Thakur, A. K.; Singh, A. K.; Prakash, S.; Kulshrestha, V.; Shahi, V. K. Stable Ion-Exchange Membranes for Water Desalination by Electrodialysis. *Desalination* **2011**, *282*, 2−8.
(51) Thakur, A. K.; Gahlot, S.; Kulshrestha, V.; Shahi, V. K. Highly Stable Acid−Base Complex Membrane for Ethanol Dehydration by Pervaporation Separation. *RSC Adv.* **2013**, *3*, 22014−22022.
(52) Jiang, Z.; Zhao, X.; Fu, Y.; Manthiram, A. Composite Membranes Based on Sulfonated Poly(ether ether ketone) and SDBS-Adsorbed Graphene Oxide for Direct Methanol Fuel Cells. *J. Mater. Chem.* **2012**, *22*, 24862−24869.
(53) Hoarfrost, M. L.; Tyagi, M. S.; Segalman, R. A.; Reimer, J. A. Effect of Confinement on Proton Transport Mechanisms in Block Copolymer/Ionic Liquid Membranes. *Macromolecules* **2012**, *45*, 3112−3120.
(54) Reed, M. A. Inelastic Electron Tunneling Spectroscopy. *Mater. Today* **2008**, *11*, 46−50.

DOI: 10.1021/am506033c
ACS Appl. Mater. Interfaces 2015, 7, 264−272